Indian Journal of Pure & Applied Physics
Vol. 52, May 2014, pp. 322-329

Microscopic non-axial study of even-even $^{226-230}$Th isotopes using octupole interaction

Daya Ram, Rani Devi* & S K Khosa

Department of Physics and Electronics, University of Jammu, Jammu 180 006, India

*E-mail: rani_rakwal@yahoo.co.in

Received 2 January 2013; revised 11 November 2013; accepted 6 February 2014

The yrast spectra, quadrupole moments, octupole moments, quadrupole deformation parameters (β_2), non-axiality parameters (γ), root mean square radii for protons and neutrons, occupation probabilities, and B(E2) transition probabilities are calculated for $^{226-230}$Th in Cranked Hartree-Bogoliubov (CHB) framework. These calculations have been performed by employing one body octupole potential field added to a quadrupole-quadrupole plus pairing model of residual interaction operating in a reasonably large valence space outside the ^{164}Pb core. Our calculations reproduce qualitatively the observed yrast spectra in ^{226}Th to ^{230}Th up to spin 20^+. The calculated results indicate that the quadrupole deformation increases and non-axiality of all these nuclei decreases along the yrast states. The results of octupole moments indicate that the octupole collectivity decreases as one moves from ^{226}Th to ^{230}Th. The observed increase in deformation in going from ^{226}Th to ^{230}Th is due to the increase in the occupation of low k components of $(2g_{9/2})_\pi$ and $(1j_{15/2})_\upsilon$ orbits.

Keywords: Cranked Hartree-Bogoliubov, Yrast spectra, Occupation numbers, B(E2) transition probability

1 Introduction

The region of light actinides exhibits signs of stable octupole deformation and offers a real challenge for nuclear structure models. The level schemes of even-even positive parity bands of some thorium isotopes have been extended up to higher spin. Azmal *et al*[1]. and Cocks *et al*[2]. have studied the spectroscopy of $^{226-230}$Th isotopes by using multi-nucleon transfer reactions. They systematically studied the rotational alignment properties of thorium isotopes and revealed the information concerning the role of the octupole phonon and the onset of stable octupole deformation with increasing rotational frequency. The difference in alignment between the positive and negative parity bands in thorium nuclei shows that ^{228,230}Th behave like octupole vibrators, in contrast with ^{226}Th which is octupole-deformed in character.

On the theoretical side, a variety of approaches have been applied to investigate the role of octupole degrees of freedom in actinide mass region. Zamfir and Kusnezov[3] studied even-even Ra-Th nuclei in the framework of the *spdf* interacting boson model and found that while the properties of the low-lying states can be understood without stable octupole deformation, higher spin states (I≥12) in some of these nuclei suggest that the octupole deformation develops with increasing spin. Diab[4] investigated the low-lying collective levels in $^{224-234}$Th in the framework of the interacting boson approximation (IBA-1) and successfully reproduced the ground state and octupole bands. Bizetti and Sona[5] investigated the nuclear octupole and quadrupole excitations close to axial symmetry in the thorium isotopic mass chain. They predicted a phase transition in the octupole mode around a stable quadrupole deformation. In the present paper, the octupole degree of freedom in the pairing-plus quadrupole–quadrupole model of interaction to investigate the yrast bands of $^{226-230}$Th, has been incorporated.

The results are obtained for the yrast states, intrinsic quadrupole moments, quadrupole deformation parameter (β_2), intrinsic octupole moments, non-axiality parameter (γ), root mean square radii for protons (r_π) and neutrons (r_υ), occupation probabilities and B(E2) transition probabilities. For the variational calculation of the yrast levels, we have employed the pairing plus quadrupole-quadrupole interaction operating in a reasonably large valence space spanned by $3p_{1/2}$, $3p_{3/2}$, $2f_{5/2}$, $2f_{7/2}$, $2g_{9/2}$, $1h_{9/2}$, $1i_{11/2}$, $1i_{13/2}$, and $1j_{15/2}$ orbits for protons as well as neutrons. The nucleus ^{164}Pb is considered as an inert core.

2 Theoretical Framework

2.1 One and two body parts of the Hamiltonian

The single particle energies (SPEs) that we have employed are (in MeV) $(2f_{7/2})$=0, $(1h_{9/2})$=0.5, $(1i_{13/2})$=1.9, $(3p_{3/2})$=2.4, $(2f_{5/2})$=2.9, $(3p_{1/2})$=3.9,

$(2g_{9/2})$=5.8, $(1i_{11/2})$=7.5, and $(1j_{15/2})$=7.8. This set of input SPEs is taken from Nilsson diagram[6]. Apart from this, one-body octupole force field is generated by the potential:

$$V_{OCT} \propto \sum_{ij} \left\langle i \left| \sum_{\mu=-3}^{+3} (-1)^{\mu} r^3 Y_{3,\mu}(\theta,\phi) \right| j \right\rangle a_i^{\dagger} a_j \qquad \ldots(1)$$

The two-body effective interaction that we have employed is pairing-plus quadrupole-quadrupole (qq) type[7]. The pairing part can be written as:

$$V_P = -(G/4) \sum_{ij} S_i S_j a_i^{\dagger} a_{\bar{i}}^{\dagger} a_{\bar{j}} a_j \qquad \ldots(2)$$

where i denotes the quantum numbers ($nljm$). The state $\bar{i}$ is same as i but with the sign of m reversed. Here S_i is the phase factor $(-1)^{j-m}$. The q-q part of the interaction is given by:

$$V_{qq} = -\frac{\chi}{2} \sum_{ijkl} \sum_{\upsilon} \left\langle i \left| q_{\upsilon}^2 \right| k \right\rangle \left\langle j \left| q_{-\upsilon}^2 \right| l \right\rangle (-1)^{\upsilon} a_i^{\dagger} a_j^{\dagger} a_l a_k \qquad \ldots(3)$$

where the operator q_{υ}^2 is given by:

$$q_{\upsilon}^2 = \left(\frac{16\pi}{5} \right)^{\frac{1}{2}} r^2 Y_{\upsilon}^2(\theta,\phi) \,. \qquad \ldots(4)$$

The strengths of interaction parameters of the like-particle neutron-neutron (χ_{nn}) or proton–proton (χ_{pp}) and the neutron–proton (χ_{np}) have been parametrized by the relations[8]:

$$\chi_{nn} \left(= \chi_{pp} \right) = -(10-11) \times \mathrm{A}^{-1.4} \,\mathrm{MeV\ a}^{-4} \qquad \ldots(5)$$

$$\chi_{np} = 1.7 \times \chi_{nn} \left(= \chi_{pp} \right) \qquad \ldots(6)$$

with G = (18-21)/A.
Here $a(=\sqrt{\hbar / m\omega})$ is the oscillator parameter.

2.2 Review of CHB Theory

All that can be done here now is to put together the important definitions and formulae which are often used.
Consider the many-body Hamiltonian :

$$H = \sum_i \langle i \,|\, T \,|\, i \rangle a_i^{\dagger} a_i + \frac{1}{4} \sum_{ijkl} \left\langle i, j \left| V_A \right| k, l \right\rangle a_i^{\dagger} a_j^{\dagger} a_l a_k \qquad \ldots(7)$$

where T is the kinetic energy and one body part of the Hamiltonian and V_A is an effective nucleon-nucleon interaction. The indices '$ijkl$' span the active valence single-particle states contained in the model space, and $a_i^{\dagger}$ and a_i are the particle creation and annihilation operators, respectively.

The cranking model for number non-conserving wave functions replaces H by:

$$H' = H - \lambda N - \omega J_x \qquad \ldots(8)$$

where the angular frequency ω is adjusted so that:

$$\left\langle J_x \right\rangle = \sqrt{J(J+1)} \qquad \ldots(9)$$

and the chemical potential λ is adjusted so that the number operator N has the correct expectation value.
The quasi-particle transformations:

$$q_i^{\dagger} = \sum_j (U_{ij} a_j^{\dagger} + V_{ij} a_j) \qquad \ldots(10)$$

are chosen so that :

$$H' = E_0' + \sum_i E_i q_i^{\dagger} q_i + H_{int} \qquad \ldots(11)$$

where E_i are the quasi-particle energies and H_{int} is the neglected quasi-particle interaction. Eqs (8) and (11) result in the HB equations appropriate for a rotating frame:

$$\begin{pmatrix} X - \omega J_x & \Delta \\ -\Delta^* & -(X - \omega J_x)^* \end{pmatrix} \begin{pmatrix} U \\ V \end{pmatrix} = E \begin{pmatrix} U \\ V \end{pmatrix} \qquad \ldots(12)$$

This energy matrix is referred to as HB Hamiltonian. The Hartree Hamiltonian, the Hartree potential and the pair potential are defined by:

$$X_{ij} = (T - \lambda + \Gamma)_{ij} \qquad \ldots(13)$$

$$\Gamma_{ij} = \sum_{kl} \langle ik \,|\, V_A \,|\, jl \rangle \rho_{lk} \qquad \ldots(14)$$

$$\Delta_{ij} = \frac{1}{2} \sum_{kl} \langle ij \,|\, V_A \,|\, kl \rangle t_{kl} \qquad \ldots(15)$$

The density matrix and the pairing tensor are:

$$\rho_{ij} = \left\langle \phi_0 \,|\, a_j^{\dagger} a_i \,|\, \phi_0 \right\rangle = (V^{\dagger} V)_{ij} \qquad \ldots(16)$$

$$t_{ij} = \left\langle \phi_0 \left| a_j a_i \right| \phi_0 \right\rangle = (V^{\dagger} U)_{ij} \qquad \ldots(17)$$

where $|\phi_0\rangle$ is the quasi-particle vacuum.

The Hamiltonian in a rotating frame contains Cranking term $-\omega J_x$ which violates many of the symmetries of Eq. (7), consequently the densities calculated from the Cranking Hamiltonian given in Eq. (8) are neither time reversal invariant nor triaxiality symmetric. Therefore, The CHB Hamiltonian will not be block diagonal if it is expressed in the spherical single-particle basis $|k\rangle=|nljm\tau\rangle$. No reduction in the dimension of the eigen value equation occurs and the solution of CHB equations becomes a formidable task. It was, however, Goodman[9] who suggested several simplifications, which result, provided one exploits certain symmetries associated with the J_x operator. It is convenient to separate the Harmonic oscillator states into two sets. The first set contains the states $\left|\mathrm{k}\right\rangle$, which are restricted to have $\left(m_k-\frac{1}{2}\right)$ equal to an even integer. The second set contains the time reversed set $\left|\bar{\mathrm{k}}\right\rangle\equiv T\left|\mathrm{k}\right\rangle$, which have $\left(m_k-\frac{1}{2}\right)$ equal to an odd integer. The symmetries preserved by $\hat{J}_x$ are parity, reflection through yz plane and rotation of π about the x-axis. Since $\sigma_x=\mathrm{PR}_x(\pi)$, only two of these symmetries, are independent. If the conventional $\left|jm\right\rangle$ basis is used, then the reflection symmetry σ_x does not reduce the dimension of the CHB equations. To take advantage of the symmetry σ_x, Goodman[9] introduced a single particle basis that simultaneously block diagonalizes the J_x term and the Hartree and pair potentials. Since $\sigma_x^2=-1$ when acting on one fermion states, the operator σ_x has only two eigen values, $-i$ and $+i$ with corresponding sets of eigen vectors that are denoted by $\left|\mathrm{K}\right\rangle$ and $\left|\bar{\mathrm{K}}\right\rangle$. Because σ_x and $\hat{J}_x$ are commuting normal operators, it follows that there are no non-zero matrix elements of $\hat{J}_x$ between eigen states of σ_x belonging to different eigenvalues of σ_x. That is:

$$\langle \mathrm{K}|J_x|\bar{\mathrm{K}}'\rangle=0 \qquad \ldots(18)$$

The eigen vectors are easily determined, since σ_x in the two-dimensional basis $\left|\mathrm{K},\bar{\mathrm{K}}\right\rangle$ has the representation:

$$\sigma_x=-i\begin{pmatrix}0 & 1\\ 1 & 0\end{pmatrix}$$

so that the eigen vectors are:

$$\left|\mathrm{K}\right\rangle=\frac{1}{\sqrt{2}}\left[\left|\mathrm{k}\right\rangle+\left|\bar{\mathrm{k}}\right\rangle\right] \qquad \ldots(19a)$$

$$\left|\bar{\mathrm{K}}\right\rangle=\frac{1}{\sqrt{2}}\left[-\left|\mathrm{k}\right\rangle+\left|\bar{\mathrm{k}}\right\rangle\right] \qquad \ldots(19b)$$

Notice that $\left|\bar{\mathrm{K}}\right\rangle=T\left|\mathrm{K}\right\rangle$. Since J_x and T anti-commute, it follows that:

$$\left\langle \mathrm{K}|J_x|\mathrm{K}'\right\rangle=-\left\langle \mathrm{K}|J_x|\mathrm{K}'\right\rangle \qquad \ldots(20)$$

thus J_x is block diagonal in the σ_x. basis $\left|\mathrm{K}_1,\mathrm{K}_2,\ldots,\mathrm{K}_N,\bar{\mathrm{K}}_1,\bar{\mathrm{K}}_2,\ldots\bar{\mathrm{K}}_N\right\rangle$

$$J_x=\begin{pmatrix}j_x & 0\\ 0 & -j_x\end{pmatrix} \qquad \ldots(21)$$

If the quasi-particle operators are chosen as:

$$q_i^\dagger=\sum_K\left(U_{iK}a_K^\dagger+V_{iK}a_{\bar{\mathrm{K}}}\right) \qquad \ldots(22)$$

$$q_{\bar{i}}^\dagger=\sum_K\left(\tilde{U}_{iK}a_{\bar{K}}^\dagger+\tilde{V}_{iK}a_K\right) \qquad \ldots(23)$$

it can then be demonstrated that the CHB equations reduce to the form:

$$\begin{pmatrix}X_1-\omega j_x & \Delta_1\\ -\Delta_1^\dagger & -(X_2+\omega j_x)^*\end{pmatrix}\begin{pmatrix}\vec{U}_i\\ \vec{V}_i\end{pmatrix}=E_i\begin{pmatrix}\vec{U}_i\\ \vec{V}_i\end{pmatrix} \qquad \ldots(24)$$

$$\begin{pmatrix}(X_2+\omega j_x)^* & \Delta_1^\dagger\\ \Delta_1 & -(X_1-\omega j_x)\end{pmatrix}\begin{pmatrix}\vec{\tilde{U}}_i^*\\ -\vec{\tilde{V}}_i^*\end{pmatrix}=\tilde{E}_i\begin{pmatrix}\vec{\tilde{U}}_i^*\\ -\vec{\tilde{V}}_i^*\end{pmatrix} \qquad \ldots(25)$$

where X now includes the Fermi energy λ. Goodman[9] demonstrated that if self-consistent symmetry σ_x is employed, the HB quasi-particle vacuum at any angular velocity may be written as:

$$\left|\phi_0\right\rangle=\prod_\alpha a_\alpha^\dagger\prod_{\beta\neq\alpha}\left(U_\beta+V_\beta a_\beta^\dagger a_{\bar{\beta}}^\dagger\right)|0\rangle \qquad \ldots(26)$$

where

$$a^{\dagger}_{\beta} = \sum_{K} D_{\beta K} a^{\dagger}_{K} \qquad \ldots(27)$$

$$a^{\dagger}_{\overline{\beta}} = \sum_{K} \overline{D}_{\beta K} a^{\dagger}_{\overline{K}} \qquad \ldots(28)$$

so that $|\beta\rangle$ and $|\overline{\beta}\rangle$ are eigen vectors of σ_x with eigen values, $-i$ and $+I$, respectively.

2.3 Matrix Elements of Hatree Hamiltonian

Let $|K\rangle$ denotes a state in the 'direct' basis and $|\overline{K}\rangle$ the state in the 'conjugate' basis; that is:

$$|K\rangle = \left[|(j_\alpha, m_\alpha)\rangle + (-1)^{j_\alpha + 1/2} |(j_\alpha, -m_\alpha)\rangle \right] \equiv |+\rangle$$
$$|\overline{K}\rangle = \left[|(j_\alpha, m_\alpha)\rangle - (-1)^{j_\alpha + 1/2} |(j_\alpha, -m_\alpha)\rangle \right] \equiv |-\rangle \quad \ldots(29)$$

then the matrix elements of the Hartree potential is:

$$\Gamma_{K_1, K_2} = \sum_{\beta} \langle K_1, \beta | V | K_2, \beta \rangle$$
$$= \sum_{K_3} \sum_{K_4} \langle K_1, K_3 | V | K_2, K_4 \rangle \, \rho_{K_3, K_4} \qquad \ldots(30)$$

Denoting the Γ matrix constructed in the K-basis for protons by $\Gamma_{+,p}$ we have :

$$\Gamma_{+,p} = \sum_{K_3 K_4} \begin{bmatrix} \langle +^p \, +^p | V | +^p \, +^p \rangle \rho_{+,p} \\ + \langle +^p \, -^p | V | +^p \, -^p \rangle \rho_{-,p} \\ + \langle +^p \, +^n | V | +^p \, +^n \rangle \rho_{+,n} \\ + \langle +^p \, -^n | V | +^p \, -^n \rangle \rho_{-,n} \end{bmatrix} \qquad \ldots(31)$$

where p over + (or $-$) implies 'proton' and n implies 'neutron'

$$\langle K_1 | \rho_{+,p} | K_2 \rangle = \sum_{\beta} |V_\beta|^2 \, D^{*}_{\beta K_1} D_{\beta K_2} \qquad \ldots(32)$$

2.4 Pairing Matrix Element

The pairing matrix element is:

$$\langle \beta_1, \overline{\beta}_1 | V_p | \beta_2 \, \overline{\beta}_2 \rangle = \sum_{K_1} D_{\beta_1 K_1} \sum_{K_2} D_{\overline{\beta}_1 K_2} \sum_{K_3} D_{\beta_2 K_3}$$
$$\times \sum_{K_4} K 4 D_{\overline{\beta}_2 K_4} \langle K_1 \, \overline{K}_2 | V_p | K_3 \, \overline{K}_4 \rangle \qquad \ldots(33)$$

The matrix elements of the pairing interaction are given by:

$$\langle j_1 m_1, j_2 m_2 | V_p | j_3 m_3, j_4 m_4 \rangle = (-G)(-1)^{j_1 + j_3 - m_1 - m_3}$$
$$\times \delta_{j_1 j_2} \delta_{j_3 j_4} \delta_{m_2, -m_1} \delta_{m_4, -m_3}$$

Employing above equation we obtain, after some algebraic manipulations

$$\langle \beta_1, \overline{\beta}_1 | V_p | \beta_2, \overline{\beta}_2 \rangle = -G \left(\sum_{K_1} D_{\beta_1 K_1} D_{\overline{\beta}_1 \overline{K}_1} (-1)^{l_\alpha} \right)$$
$$\times \left(\sum_{K_2} D_{\beta_2 K_2} D_{\overline{\beta}_2 \overline{K}_2} (-1)^{l_\alpha} \right) \qquad \ldots(34)$$

where $|K_1\rangle$ is given by Eq. (29)

3 Results and Discussion

3.1 Results of calculation for $^{226-230}$Th isotopes

In Table 1, the results of CHB calculation using pairing plus quadrupole-quadrupole model are presented. The values for the two components of quadrupole moments $\langle Q_0^2 \rangle$ and $\langle Q_2^2 \rangle$ are presented separately for protons and neutrons. It turns out from our calculation that $\langle Q_{-2}^2 \rangle = \langle Q_2^2 \rangle$ and $\langle Q_1^2 \rangle = \langle Q_{-1}^2 \rangle = 0$. From Table 1, it is observed that the $\langle Q_0^2 \rangle_{\pi,\upsilon}$ values show an increase as one moves along the yrast states for a particular nucleus. Besides this, these values also show an increasing trend with increase in neutron number. However, the trend exhibited by $\langle Q_2^2 \rangle_{\pi,\upsilon}$ values for a particular nucleus as one moves up along the yrast states is decreasing. It is observed from the columns 4th and 6th of Table 1 that for $^{226-230}$Th, the $\langle Q_2^2 \rangle_{\pi}$ values show a slow decrease along the yrast states as well as with neutron number whereas, the $\langle Q_2^2 \rangle_{\upsilon}$ values show an increase with neutron number. The values of β_2 presented in Table 1 are calculated from the values of intrinsic quadrupole moments by using the standard formula suggested by Bohr[10]. The values of β_2 parameter for $^{226-230}$Th are 0.216, 0.227, 0.228 that are found to be in satisfactory agreement with the values 0.228(7), 0.2301(39), 0.2441(15), respectively, adopted by

Table 1 — Results of CHB calculations for $^{226\text{-}230}$Th. Here $\langle Q_0^2\rangle_\pi$ $\left(\langle Q_0^2\rangle_\nu\right)$, $\langle Q_2^2\rangle_\pi\left(\langle Q_2^2\rangle_\nu\right)$ and $\langle Q_1^3\rangle_\pi$ $\left(\langle Q_1^3\rangle_\nu\right)$, $\langle Q_3^3\rangle_\pi$ $\left(\langle Q_3^3\rangle_\nu\right)$ gives the contribution of the protons (neutrons) to the components of quadrupole and octupole moment operators,respectively. The quadrupole and octupole moments are calculated in units of 'b' and '$b^{3/2}$', respectively, where b is barn. The 11th column gives the calculated and adopted values of quadrupole deformation parameter (β_2). The adopted values are given in square bracket and taken from Ref.11. The 12th column gives the value γ, the degree of non-axiality. The values $r_\pi(r_\upsilon)$ given in columns 13th and 14th are the root mean square radii for protons (neutrons) in fermis

Nuclei	I	$\langle Q_0^2\rangle_\pi$	$\langle Q_2^2\rangle_\pi$	$\langle Q_0^2\rangle_\nu$	$\langle Q_2^2\rangle_\nu$	$\langle Q_1^3\rangle_\pi$	$\langle Q_3^3\rangle_\pi$	$\langle Q_1^3\rangle_\nu$	$\langle Q_3^3\rangle_\nu$	β_2	γ	r_π	r_υ
										[0.228(7)]			
^{226}Th	0	2.18	1.08	2.96	3.35	0.025	0.021	0.053	0.088	0.216	-58.93	6.47	6.62
	2	2.18	1.08	2.96	3.35	0.025	0.022	0.053	0.087		-58.86	6.49	6.62
	4	2.19	1.08	2.96	3.34	0.025	0.023	0.052	0.085		-58.69	6.51	6.62
	6	2.20	1.07	2.96	3.34	0.025	0.023	0.052	0.084		-58.45	6.53	6.62
	8	2.21	1.06	2.96	3.32	0.025	0.024	0.051	0.082		-58.15	6.55	6.62
	10	2.23	1.05	2.97	3.31	0.025	0.024	0.051	0.080		-57.78	6.57	6.62
	12	2.25	1.04	2.97	3.29	0.025	0.024	0.050	0.079		-57.37	6.59	6.62
	14	2.26	1.03	2.98	3.27	0.025	0.025	0.050	0.077		-56.90	6.61	6.63
	16	2.27	1.01	2.98	3.25	0.025	0.025	0.049	0.075		-56.47	6.62	6.63
	18	2.28	1.00	2.99	3.23	0.025	0.025	0.049	0.073		-55.92	6.64	6.63
	20	2.30	0.98	3.00	3.19	0.026	0.025	0.049	0.071		-55.43	6.65	6.63
										[0.2301(39)]			
^{228}Th	0	2.48	0.99	3.29	3.52	0.020	0.017	0.042	0.067	0.227	-56.59	6.47	6.65
	2	2.48	0.99	3.29	3.52	0.019	0.017	0.042	0.066		-56.56	6.49	6.65
	4	2.49	0.98	3.28	3.51	0.019	0.017	0.042	0.065		-56.45	6.51	6.65
	6	2.49	0.98	3.30	3.51	0.019	0.018	0.041	0.064		-56.28	6.53	6.65
	8	2.50	0.98	3.31	3.50	0.019	0.018	0.041	0.063		-56.01	6.54	6.65
	10	2.50	0.97	3.31	3.48	0.019	0.018	0.041	0.061		-55.77	6.56	6.65
	12	2.51	0.97	3.32	3.47	0.019	0.019	0.041	0.060		-55.47	6.57	6.65
	14	2.52	0.96	3.33	3.45	0.019	0.019	0.041	0.058		-55.11	6.59	6.65
	16	2.53	0.96	3.34	3.45	0.019	0.019	0.041	0.057		-54.71	6.60	6.65
	18	2.54	0.95	3.36	3.43	0.019	0.019	0.041	0.055		-54.30	6.61	6.65
	20	2.55	0.94	3.37	3.40	0.019	0.020	0.041	0.053		-53.74	6.62	6.65
										[0.2441(15)]			
^{230}Th	0	2.78	0.88	4.04	3.97	0.020	0.017	0.040	0.066	0.228	-49.97	6.50	6.69
	2	2.79	0.87	4.08	3.40	0.020	0.017	0.039	0.064		-49.96	6.51	6.70
	4	1.80	0.87	4.15	3.41	0.020	0.017	0.039	0.062		-49.92	6.52	6.70
	6	2.81	0.87	4.21	3.41	0.022	0.017	0.038	0.058		-49.86	6.53	6.70
	8	2.82	0.86	4.30	3.41	0.022	0.017	0.037	0.053		-49.70	6.53	6.70
	10	2.84	0.85	4.41	3.40	0.022	0.017	0.036	0.045		-49.64	6.54	6.70
	12	2.84	0.85	4.41	3.38	0.022	0.017	0.036	0.044		-49.57	6.54	6.70
	14	2.84	0.85	4.42	3.37	0.022	0.017	0.035	0.042		-49.43	6.55	6.70
	16	2.84	0.84	4.43	3.36	0.022	0.017	0.035	0.041		-49.26	6.57	6.70
	18	2.84	0.84	4.43	3.34	0.022	0.017	0.034	0.039		-49.07	6.57	6.70
	20	2.84	0.84	4.43	3.33	0.022	0.017	0.034	0.038		-48.83	6.56	6.70

Raman *et al*[11]. The values for the two components of octupole moments $\langle Q_3^3\rangle$ and $\langle Q_1^3\rangle$ are presented separately for protons and neutrons. It turns out from our calculations that $\langle Q_{-3}^3\rangle=\langle Q_3^3\rangle$ and $\langle Q_{-1}^3\rangle=\langle Q_1^3\rangle$ and $\langle Q_{-2}^3\rangle=\langle Q_2^3\rangle$ $=\langle Q_0^3\rangle=$ 0. From Table 1, it is observed that $\langle Q_{3,1}^3\rangle_{\pi,\upsilon}$ values show a decrease as one moves from ^{226}Th to ^{230}Th, predicting thereby decrease in octupole collectivity with neutron number that is consistent with the experimental observations[1,2,12-15]. So, the present CHB results with octupole interaction predict $^{226\text{-}230}$Th to have octupole collectivity. The parameter γ is a measure of the degree of non-axiality present in a nucleus. The values of γ are calculated from the $\langle Q_2^2\rangle$ values by

Table 2 — Values of occupation probabilities of the ground state for $^{226\text{-}230}$Th

Nucleus	$3p_{1/2}$	$3p_{3/2}$	$2f_{5/2}$	$2f_{7/2}$	$2g_{9/2}$	$1h_{9/2}$	$1i_{11/2}$	$1i_{13/2}$	$1j_{15/2}$
					Protons				
^{226}Th	0.17	0.85	0.35	2.50	0.02	2.13	0.001	1.98	0.001
^{228}Th	0.28	0.80	0.55	2.26	0.07	2.08	0.004	1.93	0.007
^{230}Th	0.37	0.84	0.73	2.08	0.20	1.97	0.002	1.80	0.001
					Neutrons				
^{226}Th	1.35	3.52	5.31	7.89	5.11	9.91	4.15	12.74	4.01
^{228}Th	1.42	3.49	5.33	7.86	5.38	9.89	4.28	12.33	6.00
^{230}Th	1.43	3.10	4.75	7.57	6.01	9.58	5.87	12.37	7.29

using the formula suggested by Bohr[10] and these values show a decrease with spin and neutron number. In the last two columns of Table 1, the root mean square radii for protons and neutrons are presented. It can be seen that the values of r_υ are almost constant along the yrast states whereas r_π values show a slight increase as one moves along the yrast states. Thus, the results on $\left\langle Q_0^2 \right\rangle_{\pi,\upsilon}$ and γ show that axial quadrupole collectivity increases and non-axiality decreases for these nuclei in going up along the yrast states. The results on octupole moments seem to predict that octupole collectivity is maximum for ^{226}Th then it shows a decrease as one moves from ^{226}Th to ^{230}Th.

3.2 Subshell occupation number

In Table 2, the subshell occupation numbers for protons and neutrons are presented. A careful examination of Table 2 shows that the occupation numbers of various proton orbits are spread over $3p_{1/2}$, $3p_{3/2}$, $2f_{5/2}$, $2f_{7/2}$, $2g_{9/2}$, $1h_{9/2}$, $1i_{11/2}$, $1i_{13/2}$ and $1j_{15/2}$ orbits. Here the occupation probabilities of $3p_{1/2}$, $2f_{5/2}$ and $2g_{9/2}$ orbits increase whereas the occupation probabilities of $2f_{7/2}$, $1h_{9/2}$ and $1i_{13/2}$ orbits show a slow decrease as one moves from ^{226}Th to ^{230}Th. The increase in the occupation of $(2g_{9/2})_\pi$ orbit from 0.02 to 0.20 causes an increase in deformation in going from ^{226}Th to ^{230}Th.

In case of occupation numbers for neutrons, the occupation probability of $1j_{15/2}$ orbit increases from 4.01 to 7.29 units as one moves from ^{226}Th to ^{230}Th causing thereby an increase in quadrupole deformation. This increase in quadrupole deformation is also observed experimentally as the energy of $E_{2_1^+}$ decreases to a value of 0.053 MeV in ^{230}Th from its value of 0.072 MeV in ^{226}Th.

Table 3 — Comparison of theoretical and experimental $B(E2;0_1^+ \to 2_1^+)$ values in $^{226\text{-}230}$Th.

Nucleus	$B(E2;0_1^+ \to 2_1^+)$ (in e^2b^2)	
	Exp.	Th.
^{226}Th	6.85(42)[a]	6.16
^{228}Th	7.06(24)[a]	6.89
^{230}Th	8.20(25)[b]	7.03

[a]Data is taken from Ref.11
[b]Data is taken from Ref.17

3.3 B(E2) transition probabilities

We have examined the goodness of the CHB wave function by calculating the $B\left(E2;0_1^+ \to 2_1^+\right)$ values. It has been shown[16] that the B(E2) values are related to the deformation parameter β_2 by the relation:

$$B\left(E2;0_1^+ \to 2_1^+\right) = \left[\frac{3Z \times R_0^2}{4\pi}\right]^2 \times \beta_2^2$$

where R_0 is 1.2 $A^{1/3}$ fm and B(E2) values are in units of e^2b^2.

In Table 3, a comparison of the observed $B\left(E2;0_1^+ \to 2_1^+\right)$ values with the calculated ones is presented by substituting in above relation the non-axial values of β_2 for $^{226\text{-}230}$Th given in Table 3. Here the effective charge is taken as *Z/A* i.e effective charge of proton (e_π) is (1+*Z/A*) and effective charge of neutron (e_υ) is *Z/A*. From Table 1, one notes that the calculated $B(E2;0_1^+ \to 2_1^+)$ values of $^{226\text{-}228}$Th reproduce the experimental values within experimental error limits.

3.4 Yrast spectra

In Fig. 1, the yrast spectrum of $^{226\text{-}230}$Th calculated up to spin $I=20^+$ is compared with the experimental data[1,2,17]. It is observed that the experimental yrast

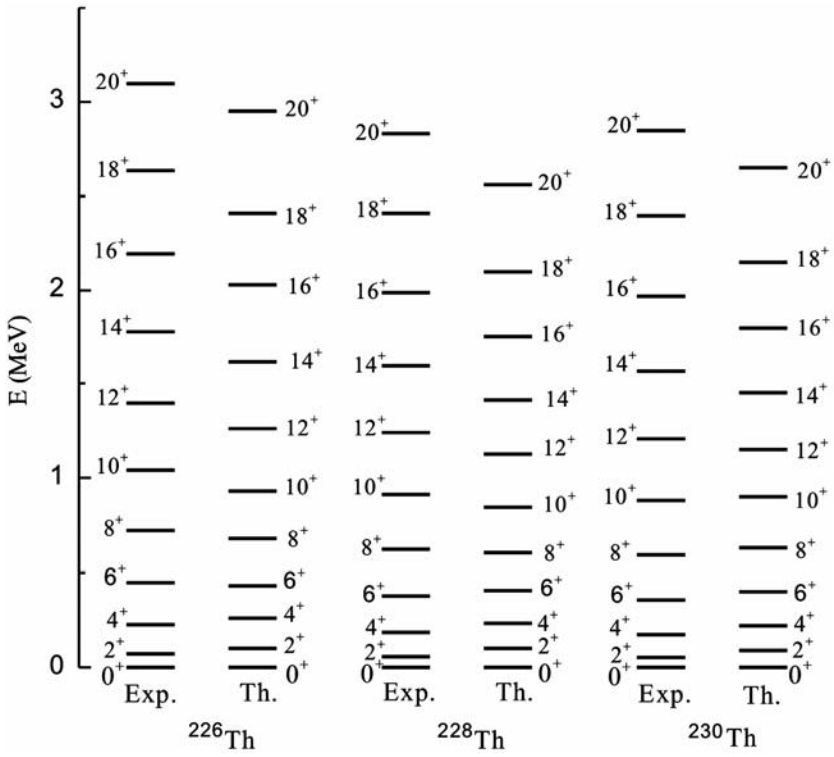

Fig. 1 — Comparison of experimental and calculated yrast spectra for $^{226\text{-}230}$Th. The experimental data is taken from Refs (1, 2, 17)

energies are reproduced well up to spin I=20^+ for $^{226\text{-}230}$Th, respectively. The experimental value of E_{20^+} of $^{226\text{-}230}$Th are 3.08 MeV, 2.83 MeV, 2.84 MeV and their theoretical values are 2.96 MeV, 2.56 MeV and 2.48 MeV, respectively.

4 Conclusions

To summarize, the CHB calculations performed by employing one body octupole potential field added to a quadrupole-quadrupole plus pairing model of residual interaction operating in a reasonably large valence space outside the ^{164}Pb core appear to give a good description of positive parity yrast states of even-even $^{226\text{-}230}$Th isotopes. It confirms theoretically the non-axial and octupole nature of these isotopes. It is found that the quadrupole deformation increases and non-axiality of all these nuclei decreases along the yrast states. From the results of octupole moments, one infers that the octupole collectivity decreases as one moves from ^{226}Th to ^{230}Th. From the results of occupation numbers, it is found that the increase in collectivity as one moves from ^{226}Th to ^{230}Th could be linked with an increase in the occupation of $(2g_{9/2})_\pi$ and $(1j_{15/2})_\upsilon$ orbits. The observed deformation increase in going from ^{226}Th to ^{230}Th is due to increase in the occupation of $(1j_{15/2})_\upsilon$ orbit from 4.02 to 7.29 and the increase in the occupation of $(2g_{9/2})_\pi$ orbit from its value of 0.02 to 0.20. The experimental B(E2) transition probabilities are reproduced for $^{226\text{-}228}$Th by taking the value of effective charge as *Z*/*A*.

Acknowledgement

One of the authors (DR) is grateful to University Grants Commission (UGC), New Delhi, India, for providing financial assistance under RGNSRF No. F. 16-1702(SC)/2010(SA-III).

References

1 Azmal N, Cocks J F C, Butler P A *et al.*, *J Phys: G Nucl & Particle Phys,* 25 (1999) 831.
2 Cocks J F C, Hawcroft D, Amzal N *et al.*, *Nucl Phys*, A645 (1999) 61.
3 Zamfir N V & Kusnezov D, *Phys Rev*, C63 (2001) 054306.
4 Diab S M, *Progress In Phys*, 2 (2008) 97.
5 Bizzeti P G & Bizzeti-Sona A M, *Phys Rev*, C70 (2004) 064319.
6 http://ie.lbl.gov/toipdf/nilsson.pdf
7 Baranger M & Kumar K, *Nucl Phys*, A110, (1968) 490.
8 Ram D, Devi R & Khosa S K, *Braz J. Phys,* 43 (2013) 247.
9 Goodman A L, *Nucl Phys*, A230 (1974) 466.

10 Bohr A, *K Dan Vidensk Selsk Mat Fys Medd*, 14 (1952) 26.
11 Raman S, Nestor Jr C W & Tikkanen P, *At Data and Nuclear Data Tables*, 78 (2001) 1.
12 Liag C F, Paris P, Sheline R K, Trubert D, Naour C L & Vergnes M, *Phys Rev*, C57 (1998) 1145.
13 Hardt K, Schuler P, Gunther C, Recht J, Blume K P & Wilzek H, *Nucl Phys*, A419 (1984) 34.
14 Kurcewicz W, *Hyperfine Interactions*, 129 (2000) 175.
15 Groger J, Weber T, De Boer J, Baltzer H, Freitag K, Gollwitzer A, Graw G & Gunther C, *Acta Physica Polonica*, 29 (1998) 365.
16 Raman S, Nestor Jr C W, *Phys Rev C* 37 (1988) 805.
17 Browne E & Tuli J K, *Nuclear Data Sheets*, 113 (2012) 2113.